Core testing method to assess nonlinear shear-sliding behaviour of brick-mortar interfaces A comparative experimental study

Jafari, Samira; Rots, Jan; Esposito, Rita

DOI
10.1016/j.conbuildmat.2020.118236

Publication date
2020

Document Version
Final published version

Published in
Construction and Building Materials

Construction and Building Materials 244 (2020) 118236

Contents lists available at ScienceDirect

Construction and Building Materials

journal homepage: www.elsevier.com/locate/conbuildmat

Core testing method to assess nonlinear shear-sliding behaviour of brick-mortar interfaces: A comparative experimental study

Samira Jafari *, Jan G. Rots, Rita Esposito

Delft University of Technology, Faculty of Civil Engineering and Geoscience, Delft, The Netherlands

HIGHLIGHTS

- Evaluating the nonlinear shear behavior of masonry by splitting tests on small cores.
- Slightly-destructive sampling method suitable for existing masonry structures.
- Good estimation of cohesion and friction coefficient on replicated/existing samples.
- Novel potential approach for providing insights into the mode-II fracture energy.
- Reliable and comprehensive alternative to conventional in-situ shear test.

ARTICLE INFO

Article history:
Received 5 August 2019
Received in revised form 19 January 2020
Accepted 21 January 2020

Keywords:
Cylindrical cores
Nonlinear shear-sliding behaviour
Post-peak softening
Slightly-destructive sampling method
Energy dissipation in shear

ABSTRACT

In this study, tests on cores and companion tests on triplets are compared with respect to the evaluation of the nonlinear shear-sliding behaviour of masonry, including the determination of post-peak softening response. Due to its slightly-destructive sampling nature and its good agreement with triplet results, the core testing method is confirmed to be a competitive technique for the in-situ assessment of the cohesion, friction coefficient, and shear modulus of mortar. Additionally, the comparisons in terms of dilatancy and energy dissipation, novel aspects with respect to previous studies, provide interesting insights for further research on the cohesive and frictional mechanisms occurring at brick-mortar interfaces.

1. Introduction

Nonlinear numerical analyses, often used for the assessment of unreinforced masonry (URM) buildings subject to earthquake and wind load, require a detailed description of nonlinear shear-sliding behaviour along the brick-mortar interface, including the evaluation of post-cracking response. In fact, different modelling approaches, such as continuum approaches (e.g. [1,2]), micromechanical-based approaches (e.g. [3,4]), and discrete models (e.g. [5,6]) postulate a constitutive law to describe this behaviour. Under a combination of axial and lateral loading, the shear failure of URM walls is characterised as a stepwise diagonal shear cracking along the head joints and bed joints, and/or a shear-sliding along the bed joint. Previous experimental studies (e.g. [7–9]) indicated that the shear resistance of a URM wall was associated with the characteristics of the masonry component, such as wall geometry, overburden, and boundary conditions, as well as with the characteristics of the masonry material. Focusing on the latter, the present paper deals with a detailed characterization of the nonlinear shear-sliding behaviour of masonry along the brick–mortar interface in terms of cohesion, friction coefficient, shear modulus of the mortar joint, fracture energy (i.e. the energy required to create one unit area of a shear crack), and dilatancy.

In view of structural assessment, the in-situ characterization of nonlinear shear-sliding behaviour at the brick mortar interface is of high relevance. Of the different standardized testing methods, shear-compression testing on triplets (Fig. 1a), prescribed by the standard EN 1052-3:2002 [10], is regarded as a suitable method. By means of standard displacement-controlled equipment, both pre- and post-peak shear properties can be determined. However, the invasive extraction of multiple samples, made of three courses of bricks, is the major drawback in the practical application of this method. As an alternative, an in-situ method which involves a minimum disturbance to wall integrity was introduced by the standard

* Corresponding author.
E-mail addresses: S.Jafari@tudelft.nl (S. Jafari), J.G.Rots@tudelft.nl (J.G. Rots), R.Esposito@tudelft.nl (R. Esposito).

https://doi.org/10.1016/j.conbuildmat.2020.118236
0950-0618/

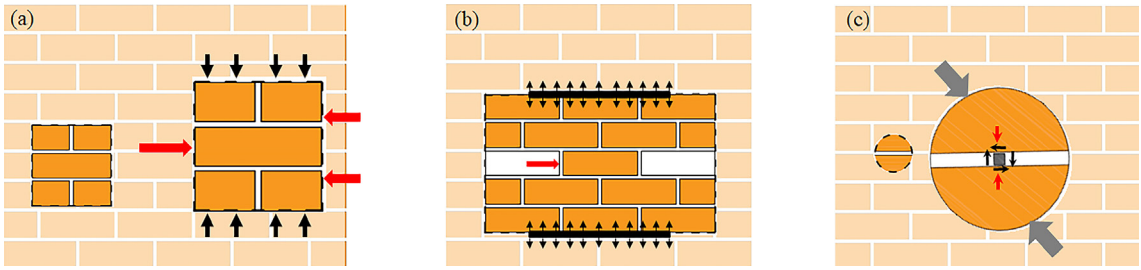

Fig. 1. Characterising shear-sliding behaviour along the brick-mortar interface using: (a) laboratory shear-compression testing on triplets; (b) in-situ shove testing on a portion of masonry wall; (c) laboratory shear testing on a small-diameter core.

ASTM C1531-16 [11], known as the "shove test" or "push test" (Fig. 1b). Different than the laboratory triplet test, the shove test allows for determining only the cohesion and friction coefficient, and it is not likely to provide information on mode-II fracture energy. To perform a shove test, specialized technical experts should continuously monitor the deformations of the masonry wall using accurate instrumentation. This should be done to prevent the unwanted cracking of the contrast portion of the wall, which could introduce uncertainty regarding the reliability of the test [12,13]. As the wall integrity is to some extent disturbed, objective interpretation of the factual normal stress acting on the tested brick due to the contribution of both flat-jacks and overburden is seldom possible [14]. In this context, by integrating numerical and experimental approaches, Andreotti et al. [15] and Ferretti et al. [16] provided better insight into the stress redistribution that occurs during the shove test. It should be pointed out that, due to the differences in the boundary conditions of the triplet test and the shove test, the accuracy of the experimental result could be argued [15,17]. Nevertheless, the drawbacks and limitations of these conventional laboratory and in-situ testing methods gave rise to the development of novel methodologies, such as tube-jack testing [18] and the core testing method [18–26].

As a minimally invasive inspection method is of paramount interest, particularly in the case of historical heritage structures, core testing was recently put forward as a novel method for characterizing the shear behaviour of brick masonry along the brick-mortar interface [18–25]. This method is based on the in-situ extraction of cylindrical cores having a diameter ranging from 70 to 100 mm and consisting of one central bed joint (Fig. 1c). In the laboratory, the cores are subjected to a vertical line load along their thickness, similar to a Brazilian splitting test [27]. By rotating the bed joint of the cores with respect to their original extraction position, different testing configurations can be considered by introducing various shear-compression stress states along the brick-mortar interface. As the loading condition is similar to that of the Brazilian splitting test, it is often referred to as a splitting test on the core. However, with reference to its purpose, the authors refer to this test as a shear test on the core. As stated by Pelà et al. [23], this method was first introduced by Braga et al. [19], who performed tests with a mortar inclination angle of 45°, aiming to reproduce a pure shear stress state along the brick–mortar interface that would be as comparable as possible to the diagonal-compression tests on panels standardized in [28]. With the aim of obtaining mortar properties, Benedetti et al. [19,21] performed tests on cores with mortar inclination angles of 30°, 45°, and 60°. In follow-up studies [21–25], extensive experimental research was performed using a mortar inclination angle between 0° and 60°. The failure mode of the cores with mortar inclination angles between 40° and 55° was predominantly described as a shear-sliding along the brick–mortar interface, enabling the calculation of the shear strength parameters in agreement with the Coulomb friction criterion [21–24]. In this context, to confirm the accuracy of the failure criterion established by the core testing method, Mazzotti et al. [22] and Pelà et al. [23] also performed shear-compression tests on companion specimens. As reported by them, the shear strength of the companion specimens, characterised in terms of cohesion (initial shear strength) and friction coefficient, matched well with the results of shear tests on cores. Accordingly, the core testing method provides basic knowledge about the shear mechanical properties (i.e. cohesion and friction coefficient) for assessing the structural response. However, for accurate predictions of the failure mechanism and failure modes of masonry structures, not only the strength at peak but also a full description of the shear properties in the pre-peak and post-peak phases is often required. It should be emphasized that the reliability of the core testing method may be questioned on the grounds that it provides insight into the local behaviour of masonry rather than the whole structure. Nevertheless, the same concern applies to all the available in-situ testing methods when a small and representative portion of masonry is tested.

In spite of the valuable contribution of previous studies on the suitability of the core testing method [18–25], the potential of this method to determine the complete nonlinear shear-sliding behaviour of masonry has not been broadly investigated (i.e. in terms of shear modulus of the mortar joint, post-peak cohesion softening behaviour, and dilatancy). In addition, previous studies focused only on clay brick masonry samples extracted from masonry that was replicated in laboratories. Thus, the possibility of offsetting the wide variation in results could be raised, as the influence of aged materials and workmanship on mechanical properties is deliberately neglected. Considering that the core testing method shows potential for in-situ characterization of masonry due to its limited sampling invasiveness and the straightforward interpretation of the testing results, this study investigates the further potentialities of the method.

To evaluate the complete nonlinear shear-sliding behaviour at the brick–mortar interface, shear tests on 69 cores and shear-compression tests on 42 companion samples were performed. In this context, seven brick masonry types, including clay and calcium silicate (CS) brick masonry, were selected for testing. The samples were extracted in the field from the load-bearing walls of four residential buildings or were made in the laboratory. A comparative experimental approach is adopted, where the progressive shear failure at the brick–mortar interface is characterised through shear tests on small-diameter cores and shear-compression tests on companion triplets. Previous findings on the suitability of the core testing method in assessing the cohesion and friction coefficient of masonry are confirmed and a larger database is provided. Considerations of the energy dissipation and dilatancy effects in the core and the triplet tests provide valuable new insights that highlight the potential of the core testing method for the in-situ characterization of masonry.

2. Experimental program

This section provides an overview of the testing scheme, including the preparation of the samples (both cores and triplets) and a detailed description of the testing procedure. The experimental program was carried out at the MacroLab/Stevin Laboratory of Delft University of Technology (TU Delft), within the framework of an extensive multi-scale testing campaign in support of the assessment and strengthening of URM buildings subject to induced seismicity in the northern part of the Netherlands [28–33].

2.1. Testing objects

The experimental program focused on extracted samples from existing buildings located in the northern part of the Netherlands, in the province of Groningen, and replicated samples built in the laboratory. Both clay and CS brick masonry were investigated, as they are the most frequently used materials in the Netherlands construction industry. In total, seven different masonry objects were included in this study (Fig. 2), as each building used for the sampling and each masonry type replicated in the laboratory were treated as separate objects.

Tests were conducted on small-diameter cores of 92–105 mm diameter having one central bed joint, as well as tests on companion triplets of one brick in length and three brick courses in height. Considering that a running bond pattern is used in existing buildings, the replicated masonry specimens were built with a running bond pattern and are here called "modified triplets" (Fig. A.1a, Appendix A). They differ from "standard triplets" (Fig. A.1b, Appendix A) composed of stack-bonded bricks, and comply with EN 1052-3: 2002 [10]. To investigate the difference between the shear properties of standard triplets and modified triplets, both triplet configurations were built in the laboratory and tested under shear-compression loading. A summary of the shear strength of both modified and standard triplets is given in Appendix A.

Four residential buildings were selected for the extraction of both small-diameter cores and companion triplets as testing objects. In total, 36 cores and 25 modified triplets were extracted. All the buildings were made of single wythe walls with a thickness of 100 mm. In addition, to characterise the properties of the brick, 30 full bricks were extracted. It should be noted that the selection of residential buildings for sampling was primarily made in the broader context of enhancing a regional database of Dutch material properties. The database, classified according to masonry types and construction periods, was gradually augmented using testing samples extracted from 16 buildings (either in clay or CS masonry) for the construction period dating from the early 1920 s to 2005 [28,30].

To reproduce samples in the laboratory, the established Dutch database was used as a benchmark for selecting material components [28,30]. To ensure the uniform behaviour of masonry specimens, all the bricks and mortar were from the same batch. The aim was to recreate a terraced house typology with a cavity wall system resembling those built between 1960 and 1985 in the Netherlands, and a typical detached house typology with load-bearing walls either in single or double wythe from the period before 1945. The load-bearing inner leaf of the terraced house was built using CS bricks with a nominal dimension of 210 × 70 × 100-mm and a ready-mixed cement-based mortar having a volume ratio of cement to sand of 1:3. This replicated masonry type was introduced as MAT-1. The detached house was constructed using solid clay bricks with a nominal dimension of 210 × 50 × 100-mm and a ready-mixed cement-based mortar having a cement to lime to sand ratio of 1:2:9 by volume. Both single wythe walls (100 mm in thickness), introduced as MAT-3, and double wythe walls (210 mm in thickness), introduced as MAT-4, were constructed. The construction of the single wythe clay masonry wall was not in line with the objectives of the current study, and was intended for investigating the shear-compression response of masonry at a component level. However, there was an opportunity to collect cores from intact pieces of this wall after testing, as shear failure was characterised by two diagonal cracks passing through all four corners [32]. In addition to the large walls, single wythe companion triplets were built. Consistent with the triplets, the double wythe cores (MAT-4) were cut in correspondence of the collar joint (Fig. 2a).

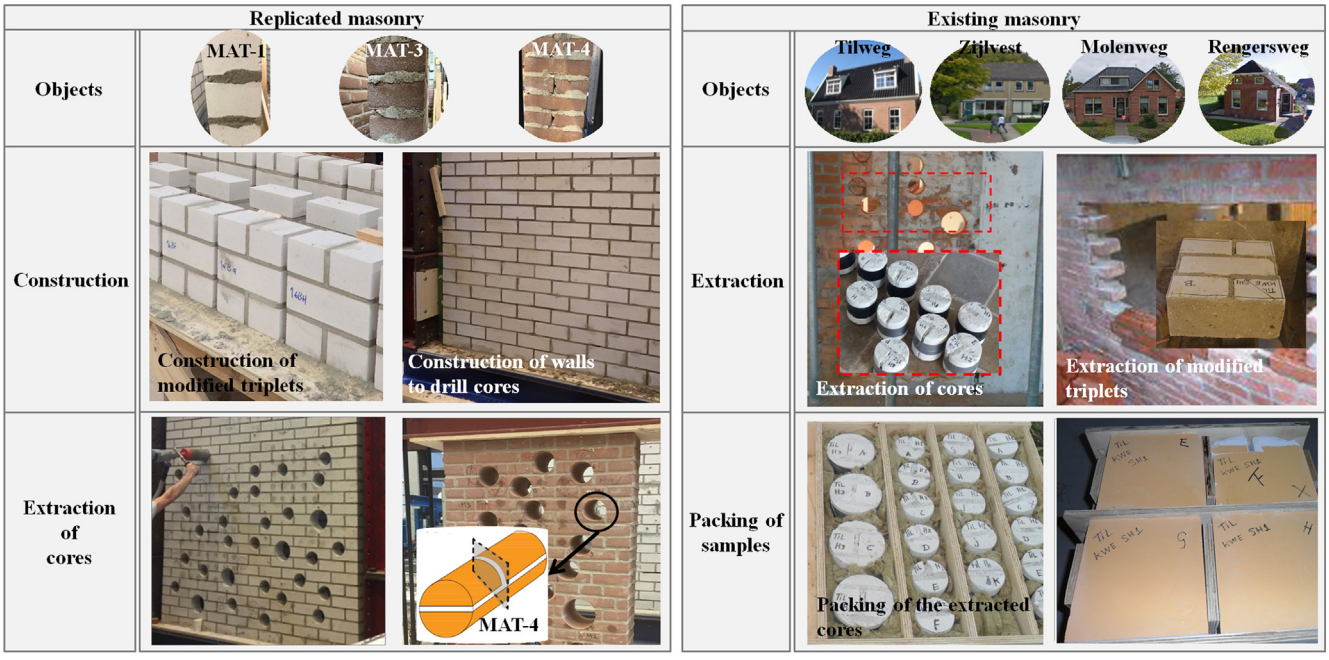

Fig. 2. Overview of the masonry objects: (a) replicated in laboratory; (b) extracted from existing buildings.

Sampling from both existing and replicated objects was performed perpendicular to the wall surface using a dry extraction procedure, as suggested by Pelà et al. [23]. Both cores and triplets were packed and transported to the laboratory according to the recommendations of the ASTM C1532 [34]. Additionally, the integrity of the replicated walls during the core drilling was a cause for safety concern in the laboratory. Hence, the walls were pre-compressed using transverse beams [23]. Note that due to the technical issues in drilling cores from the MAT-4 clay walls, in some cases, a wet extraction procedure was adopted.

Table 1 lists an overview of the tested masonry objects, and specifies the masony unit type (CS brick or solid clay), construction type (built in the laboratory or extracted from existing buildings), and the measured characteristics of masonry components in terms of compressive and flexural strength. The construction of samples in the laboratory allowed for testing the mortar properties following the standard EN 1015–11:1999 [35]. The mortar properties were measured at least 28 days after the casting of the prismatic mortar bars (160 × 40 × 40-mm) prepared during the construction of the masonry samples. However, in the case of existing objects, no intact mortar samples were obtained. Thus, enabling to perform dedicated tests for the determination of mortar compressive strength, e.g. the double punch test [24,36]. The brick properties of both replicated and existing objects were obtained by testing 12 bricks; 6 bricks were subjected to compression loading (EN 772-1:2011 [37]) and the other 6 were subjected to three-point bending (NEN 6790:2005 [38]). It is worth mentioning that cores were also extracted from the masonry objects presented in this study to determine the nonlinear compression behaviour of the masonry [39].

2.2. Testing procedure

This section describes the testing procedure adopted for the shear tests on cores and the shear-compression tests on companion triplets. The former was performed following the provisions of the literature [19–25], as no standard approach currently exists, while the latter was carried out under the guidelines of the standard EN 1052-3:2002 [10].

Under a monotonic shear load, the response of masonry cores rotated with respect to their original horizontal configuration was investigated. A load was introduced along two opposite lines, where packing strips with a density of 1099 kg/m^3 and dimensions of 194 × 15 × 2-mm were inserted between the core and the loading plates. Two different testing set-ups were used in this study, as the design of the testing procedure and measuring systems were part of the learning process. First, a displacement-controlled set-up was attempted, in which the core response was recorded by increasing the jack displacement at a rate of 0.5 μm/s. In addition to the jack displacement measurement, at each face of the core, the relative sliding of one brick portion over the other was measured using a linear variable differential transformer (LVDT) (Fig. 3a). However, due to brittle failure, the adopted set-up did not fully enable the measurement of the gradual post-peak degradation. Hence, as an alternative, a sliding-controlled set-up was adopted in which the relative sliding of the brick–mortar interface measured by the LVDTs was used as a control parameter. The sliding was increased with a rate of 0.05 μm/s. Additionally, the normal deformations perpendicular to the joints were recorded at each face using one LVDT (Fig. 3b). The LVDTs of the two testing set-ups had a measuring range of 5 mm with an accuracy of ± 1 μm.

To trigger the various combinations of shear-compression stress states along the brick–mortar interface, three different inclination angles of 45°, 50°, and 55° were used. For each inclination, when possible, at least three specimens were tested. The selection of the inclination angle was made in agreement with the observations by Mazzotti et al. [22], in which shear-sliding failure was observed for inclination angles between 40° and 50°, while unrepresentative splitting failure was observed for inclination angles less than 40° and greater than 55°. Note that for the replicated CS and clay masonry objects, tests on the cores with an inclination angle of 40° were also performed, and the failure mode was mainly reported as a shear-sliding failure along the brick–mortar interface with brick splitting failure.

The shear response of the companion triplets was investigated by subjecting a pre-compressed triplet to an increasing shear deformation along the mortar bed joints. In this study, a displacement-controlled procedure was used to apply shear load to the middle brick of a triplet at an increasing rate of 5 μm/s (Fig. 3c). The hydraulic jack had a 100 kN capacity. Throughout the test, a constant horizontal pre-compression force was applied to the specimen via a horizontal hydraulic jack that was operated manually. The horizontal jack had a 50 kN capacity and was kept in place by means of four steel rods positioned on opposite sides of the specimen, connecting two steel plates that acted as contrasts. To keep the transverse compressive load approximately constant (with an acceptable variation of ±2% [10]), a spring with a stiffness of 123 N/mm or 3300 N/mm was interposed between the actuator and the specimen. The spring with lower stiffness was used for a pre-compression level lower than 0.30 MPa, while the spring with higher stiffness was used in the other cases. The shear-compression test was repeated at three different pre-compression levels: level 1 between 0.05 and 0.35 MPa, level 2 between 0.31 and 0.70 MPa, and level 3 between 1.0 and 1.2 MPa. At each level, when possible, at least two specimens were tested. During the shear-compression tests on the modified triplets (Fig. 3c), the relative sliding of the middle brick with respect to the lateral ones was calculated as an average of the readings of all four individual vertical LVDTs. The normal displacement of the two bed joints was calculated as an average of the readings of two

Table 1
Overview of the tested masonry objects, including mortar and brick properties.

Name of objects	Wythe	Brick types	Replicated/ Existing[a]	Mortar properties[b]		Brick properties[b]		Core diameter
				Flexural strength MPa	Compressive strength MPa	Flexural Strength MPa	Compressive strength MPa	mm
MAT-1	Single	CS	Replicated	3.21 (5)	7.57 (6)	2.79 (11)	13.26 (13)	95
Tilweg	Single	CS	Existing (2000)	–	–	–	–	92
Zijlvest	Single	CS	Existing (1976)	–	–	3.53 (29)	15.90 (17)	92
MAT-3	Single	Clay	Replicated	1.40 (12)	3.81 (9)	6.31 (11)	28.31 (10)	105
MAT-4	Double							95
Molenweg	Single	Clay	Existing (1932)	–	–	2.78 (76)	21.73 (13)	92
Rengersweg	Single	Clay	Existing (1920)	–	–	–	41.90 (12)	92

(a) Year of construction of the existing building is indicated in parentheses.
(b) Coefficient of variation in percentage is indicated in parentheses.

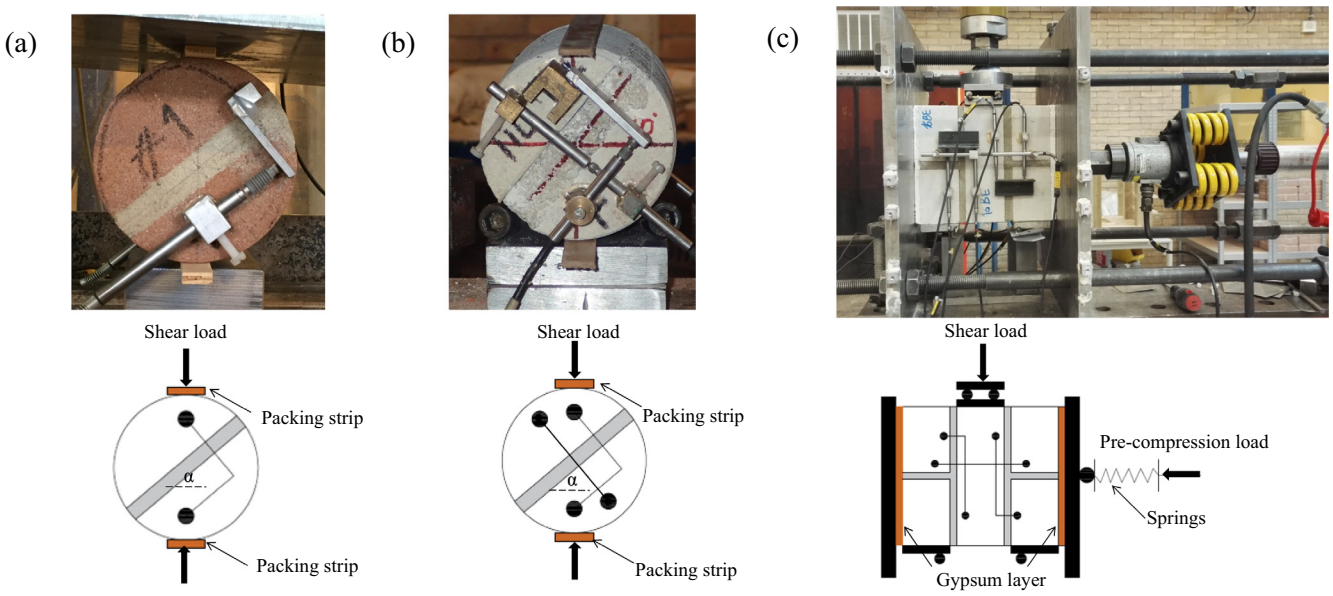

Fig. 3. Experimental set-up: (a) testing cores using displacement-controlled set-up; (b) testing core using a sliding-controlled set-up; (c) shear-compression tests on modified triplets using a displacement-controlled set-up.

horizontal LVDTs: one at each side of the triplet. The LVDTs had a measuring range of 10 mm with an accuracy of ± 5 μm.

2.3. Elaboration of experimental results

This section builds on the elaboration of the mechanical properties characterised in terms of cohesion (or initial shear strength), friction coefficient, shear modulus of the mortar joint, energy dissipation per unit area of the shear crack, and dilatancy. In the following sections, the global behaviour of cores and triplets is first presented, and thereafter, comparisons in terms of the shear properties of the two testing methods are made.

In contrast to the literature that challenged the uniform stress distribution along the brick–mortar interface, the distribution of the tangential shear stress and the normal stress was assumed to be uniform. For cores, Benedetti et al. [20] reported the local stress concentration beneath the applied load. For the triplets, it has been shown that the uniformity of the stress distribution deviates in the vicinity of the supporting plates [39–42].

For the core, the tangential shear strength ($f_{v,core}$) and the corresponding normal stress ($f_{p,core}$) associated with the maximum vertical load (F_{max}) can be estimated as follows:

$$f_{v,core} = \frac{F_{\max}.\sin\alpha}{A} \quad (1)$$

$$f_{p,core} = \frac{F_{\max}.\cos\alpha}{A} \quad (2)$$

where A is the mortar cross-sectional area, and α is the mortar inclination angle with respect to its original horizontal configuration.

For the triplet test, the shear strength (f_v) and the normal pre-compression stress (f_p) were calculated as follows:

$$f_v = \frac{F_{\max}}{2A} \quad (3)$$

$$f_p = \frac{F_h}{A} \quad (4)$$

where F_{max} is the maximum vertical load, A is the mortar cross-sectional area, and F_h is the (constant) horizontal pre-compression load.

The shear strength of both testing methods was assumed to follow the Coulomb friction criterion, as the failure modes of the cores and the triplets were characterised as a shear-sliding crack along the brick-mortar interface. Assuming a linear relation between the shear strength and the corresponding normal stress, the cohesion ($f_{v0,core}$, f_{v0}) and the friction coefficient (μ_{core}, μ) were evaluated, respectively, as the shear stress corresponding to the zero normal stress and the slope of the linear regression line (Fig. 4). For a given inclination angle, the core testing results appear along a line passing through the origin and having a slope similar to the mortar inclination (Fig. 4a). Accordingly, to exclude the effect of the number of data points, linear regression analysis was performed by considering the mean values of each inclination angle, as suggested by Mazzotti et al. [22]. For each tested object, Table 2 summarizes the cohesion and the friction coefficient obtained using the two testing methods, together with the mean values of the maximum shear stress and the corresponding normal stress.

Recording the relative sliding of the bricks allowed for the evaluation of the shear modulus of the mortar joint during the shear tests on cores and the shear-compression tests on triplets. The shear modulus of the mortar joint was determined to be the secant stiffness of the shear stress–strain curve, considering that the shear stress was calculated based on the same principal as in Eq. (1) and Eq. (3), and the strain was obtained by dividing the relative sliding by the joint thickness. Table 2 presents the values of the shear modulus evaluated in the linear-elastic phase at a stress level corresponding to 1/3 of the maximum shear stress ($G_{m,core}$, G_m). It should be noted that the sliding deformations include both the sliding of the joint as well as brick deformation. However, the brick deformation was disregarded, as the brick is much stiffer than the mortar.

In nonlinear finite element analysis of quasi-brittle materials like masonry, not only are the stiffness and strength properties reported, but so is the toughness, i.e. the post-peak softening. The toughness for shear fracture can be expressed by the mode-II fracture energy ($G_{f\text{-}II}$), which is the energy required to create a one-unit area of a shear crack along the brick–mortar interface. Nevertheless, $G_{f\text{-}II}$ cannot be simply calculated as the area underneath the shear stress-sliding curve, as the shear stress

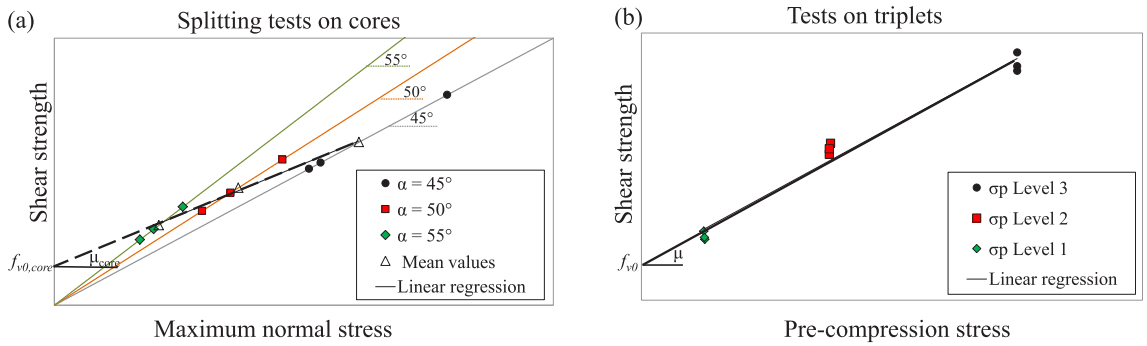

Fig. 4. Establishing failure criterion: (a) shear tests on cores; (b) shear-compression tests on triplets.

Table 2
Database of shear properties obtained from tests on cores and on companion specimens.

Objects	Shear tests on cores							Shear-compression tests on companion triplets/panels					
	α (No.)	[1]Failure (No.)	[2]$f_{v,core}$ MPa	[2]$f_{p,core}$ MPa	$f_{v0,core}$ MPa	μ_{core} –	[2]$G_{m,core}$ MPa	f_p (No.) MPa	[1]Failure (No.)	[2]f_v MPa	f_{v0} MPa	μ –	[2]G_m MPa
MAT-1	40 (4)	S (1), ST (3)	0.36 (38)	0.43 (38)	0.13	0.58	–	0.20 (3)	S (3)	0.23 (24)	0.15	0.48	290 (67)
Replicated	45 (6)	S (3), ST (3)	0.37 (25)	0.37 (25)			–	0.60 (4)	S (4)	0.46 (5)			462 (9)
CS masonry	50 (5)	S (5)	0.25 (51)	0.21 (51)			–	1.20 (3)	S (3)	0.71 (3)			402 (23)
	55 (5)	S (5)	0.22 (67)	0.22 (67)			–						
Zijlvest	45 (3)	S (1), T (2)	1.49 (-)	1.49 (-)	0.42	0.76	856 (-)	0.05 (1)	S (1)	0.32 (-)	0.29	0.79	–
Existing	50 (3)	S (2), T (1)	0.83 (19)	0.70 (19)			281 (62)	0.35 (2)	S (1), T (1)	0.63 (-)			–
CS masonry	55 (3)	S (2), ST (1)	1.10 (15)	0.77 (15)			660 (23)	0.70 (2)	S (2)	0.75 (17)			–
								1.00 (3)(3)	S (3)	1.13 (27)			–
Tilweg	45 (2)	S (2)	0.42 (3)	0.42 (3)	0.13	0.71	199 (8)	0.10 (1)	S (1)	0.18 (-)	0.12	0.62	202 (-)
Existing	50 (3)	S (2), ST (1)	0.35 (22)	0.30 (22)			226 (41)	0.31 (2)	S (2)	0.32 (3)			404 (40)
CS masonry	55 (3)	S (2), ST (1)	0.24 (21)	0.17 (21)			199 (35)	1.00 (1)	S (1)	0.74 (-)			179 (-)
MAT-3	40 (3)	ST (3)	1.33 (7)	1.58 (7)	0.22	0.80	–	0.20 (3)	S (3)	0.30 (23)	0.15	0.79	296 (27)
Replicated	45 (3)	ST (2), T (1)	0.60 (25)	0.60 (25)			–	0.60 (2)	S (2)	0.61 (11)			297 (12)
Clay masonry	50 (3)	ST (2), T (1)	1.43 (16)	1.20 (16)			–	1.00 (3)	S (3)	0.91 (11)			248 (9)
MAT-4	45 (5)	ST (4), T (1)	1.07 (32)	1.07 (32)	0.22	0.80	284 (56)						
Replicated	50 (6)	S (6)	0.50 (37)	0.42 (37)			169 (32)	The same as MAT-3					
Clay masonry	55 (6)	S (6)	0.62 (45)	0.44 (45)			162 (53)						
Molenweg[3]	45 (2)	S (1), ST (1)	1.00 (40)	1.00 (40)	0.35	0.67	1252 (44)	0.20 (3)	–	0.36 (14)	0.34	0.48	–
Existing	50 (2)	S (2)	0.90 (27)	0.76 (27)			326 (42)	0.60 (3)	–	0.79 (1)			–
Clay masonry	55 (2)	S (2)	0.63 (48)	0.44 (48)			241 (-)	1.00 (3)	–	0.73 (15)			–
Rengersweg[3]	45 (3)	ST (1), T (2)	2.47 (-)	2.47 (-)	0.49	0.85	2532 (-)	0.20 (2)	–	0.74 (12)	0.54	1.00	–
Existing	50 (3)	S (1), T (2)	0.97 (-)	0.82 (-)			496 (52)	0.40 (2)	–	0.94 (5)			–
Clay masonry	55 (3)	S (1), ST (1), T (1)	2.03 (8)	1.42 (8)			1238 (43)						–
Mazzotti [22]	40 (2)	S (1), ST (1)	1.38 (3)	1.64 (3)	0.18	0.75	–	0.23 (3)	–	0.34 (16)	0.20	0.72	–
Replicated	45 (5)	S (4), ST (1)	0.91 (15)	0.91 (15)			–	0.64 (3)	–	0.69 (4)			–
Clay masonry	50 (2)	S (2)	0.40 (7)	0.34 (7)			–	1.03 (3)	–	0.92 (8)			–
Pelà [23]	40 (5)	S (2), ST (3)	0.39 (34)	0.46 (34)	0.14	0.59	–	0.30 (3)	S (3)	0.26 (17)	0.08	0.60	–
Replicated	45 (5)	S (4), ST (1)	0.41 (11)	0.41 (11)			–	0.60 (3)	S (3)	0.45 (2)			–
Clay masonry	50 (5)	S (2), ST (3)	0.26 (20)	0.22 (20)			–	1.00 (3)	S (3)	0.68 (5)			–

Note: Calculation of mean values excluded the results of specimens with tensile failure ("T" failure mode in Fig. 6d–Fig. 7c).
[1] Letter refers to the observed failure mode, (i.e. "S" shear-sliding failure, "ST" mixed sliding along joint and tensile failure of the brick, "T" tensile failure), and the digit indicates the number of specimens having the observed failure mode.
[2] Coefficient of variation in percentage is indicated in parentheses.
[3] Tests on companion triplets were performed by third parties [46,48]; no information was available regarding the failure mode.

incorporates the contribution of both cohesive and frictional stress. In other words, the notion behind the fracture energy in shear is to distinguish the cohesion mechanism from the contribution of friction. The latter, arising from the surface roughness along the brick-mortar interface, is calculated by multiplying the friction coefficient for normal stress.

No direct comparison can be made between the shear fracture energy in the cores and in the triplets, due to the differences between them in the state of normal stress. Throughout the shear test on triplets, the pre-compression stress was kept constant, meaning that the frictional stress did not change (Fig. 5a). Accordingly, the mode-II fracture energy in the triplets was approximated as the area underneath the shear stress-sliding curve over which the cohesion decreases to zero [40,43], (Fig. 5b). The stress corresponding to the zero cohesion is known as residual shear strength, $f_{v,res}$. Unlike in the triplet test, the friction contribution was not constant throughout the shear tests on cores, as the applied load and thus the normal stress component were continuously changing. For the cores, the frictional contribution was also estimated by multiplying the friction coefficient (μ_{core}) for the normal stress component. Accordingly, the cohesive contribution was found by subtracting the frictional stress from the shear stress (Fig. 5c). The friction coefficient was evaluated by treating the results of the entire core samples together, as shown in Fig. 4a. The area underneath the cohesive stress-sliding curve could somehow reflect the dissipated energy during the shear cracking in the cores (Fig. 5d). The dissipated energy ($G_{f\text{-}core}$) was calculated only for the cores in which the pre-peak and the entire post-peak curve were

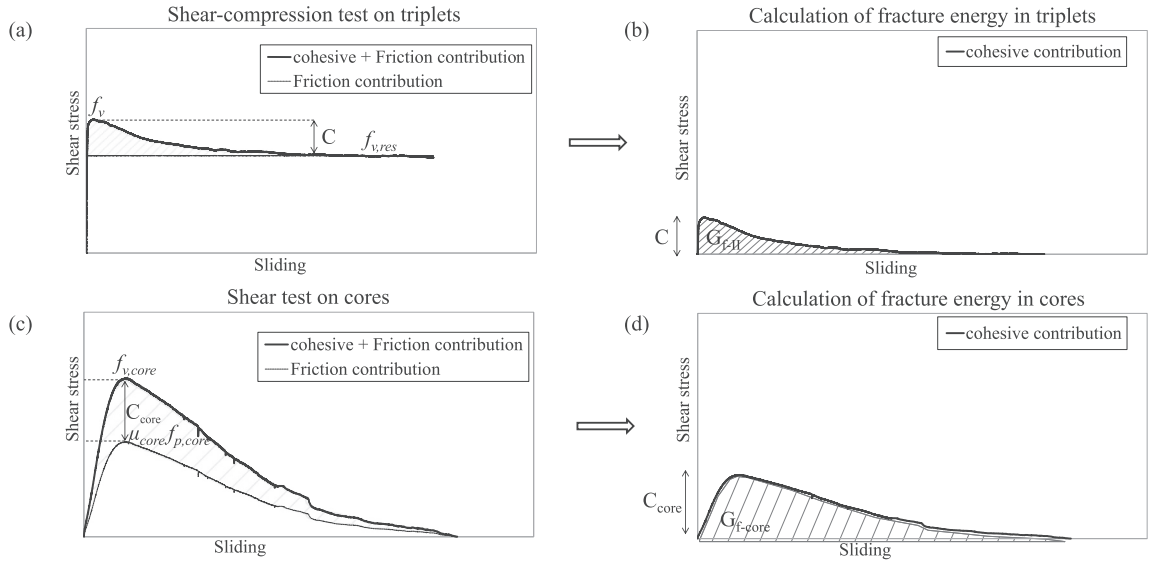

Fig. 5. Calculation of fracture energy from shear stress-sliding curves and excluding the friction contribution from the shear stress: (a,b) triplets; (c,d) cores.

successfully captured by means of the sliding-controlled set-up. As no direct comparison can be made in terms of the fracture energy of the two testing methods, Section 6 deals with predicting the post-peak response of the triplets using the results of the cores.

As supported by experimental and numerical evidence (e.g. [41–45]), when a brick-mortar interface is subjected to shear loading, upon the onset of cracking, an uplift of the joint is expected. This expansion of the joint often diminishes with larger sliding, as no further damage or degradation of asperities occurs. In confined masonry, this phenomenon, known as dilatancy, could lead to a local increase in the normal stress and thus an increase in the shear strength. Ignoring the dilatancy (i.e. assuming $\psi = 0$) often results in a non-conservative prediction of masonry response. To determine the dilatancy from the experimental results, the following formula is adopted (e.g. [43,45]):

$$\tan(\psi_{core}) = -\frac{(\eta_{pl})_{n+1} - (\eta_{pl})_n}{(\delta_{pl})_{n+1} - (\delta_{pl})_n} \quad (5)$$

where δ_{pl} is the plastic sliding displacement, η_{pl} is the corresponding plastic normal displacement perpendicular to the bed joint, and n is the increment of the sliding displacement. The calculation of the plastic displacements excludes the elastic deformation of the mortar. To this end, the mortar stiffness is assumed to be 300 times the compressive strength of mortar [46]. Note that in this study, the failure criterion is not modified to account for dilatancy.

3. Global behaviour

In this section, the global behaviour of the cores under shear load and of the triplets under combined shear-compression load is discussed and analysed. The typical final crack pattern of the cores and of the companion triplets is presented in Fig. 6 and Fig. 7, respectively. An overview of the number of cores and triplets with each specific crack pattern and typical mean shear stress-sliding curves are presented in Fig. 8. The mean shear stress-sliding curves were obtained by considering pre-defined increments of sliding and, thus, calculating the corresponding average shear stress from individual test results. In this study, an increment of the sliding equal to 1.5E−05 ± 1% was chosen. This approach was proposed by Augenti et al. [49] and had already been adopted by the authors in a previous study to find the mean compressive stress–strain curves [39].

Cores generally failed along the brick-mortar interface, but a mixed failure mode that involved the cracking of the brick was also observed in some cases. In 60% of the cases, the failure mode of the cores was characterised as a shear-sliding along one interface (Fig. 6a) or along two interfaces, including mortar cracking (Fig. 6b). Throughout the paper, this failure mode is labelled as "S". However, 25% of the total number of cores showed a combination of pure shear-sliding failure along the interface with a tensile failure of the brick(s), which appeared as a wedge-shaped splitting crack (Fig. 6c). This mode of failure was labelled as "ST". Apart from the mentioned failure modes, 15% of the total number of cores showed a predominant tensile splitting failure with a vertical tensile crack along the loading axis, rather than only shear-sliding failure along the joint (Fig. 6d). This mode of failure is introduced as "T".

Almost all triplets failed with pure shear-sliding failure either along one interface (Fig. 7a) or two interfaces (Fig. 7b), the "S" failure mode. In addition, only one triplet showed a combination of pure shear-sliding with tensile failure of the middle brick (Fig. 7c), the "T" failure mode. Neither cores nor triplets with the "T" failure mode could be regarded as representative of the shear-sliding failure along the brick-mortar interface; hence, all the mean shear properties were evaluated by excluding the outputs of these specimens. For the sake of completeness, the failure modes of all the individual specimens in terms of "S", "ST", and "T" are presented in Table 2.

Apart from the testing configuration itself, which could cause non-uniform stress distribution along the interface, the difference between the properties of the mortar relative to the brick and the quality of the bond between them could have a great influence on the stress distribution. It can be assumed that the stronger the mortar and interface, the higher the homogeneity of the material. In the case of a homogeneous material, the core is more likely to fail due to vertical splitting (such as a concrete core) than due to shear-sliding along the interface. In this study, such behaviour was more pronounced for the cores extracted from the clay masonry building of Rengersweg, where five out of nine cores clearly showed the "T" failure mode rather than the other acceptable failure modes (i.e. "S" or "ST"). Despite the replicated objects, no information was available regarding the mortar properties and the bond strength of the Rengersweg building. However, the shear properties of the triplets shown in Table 2 reveal a very high

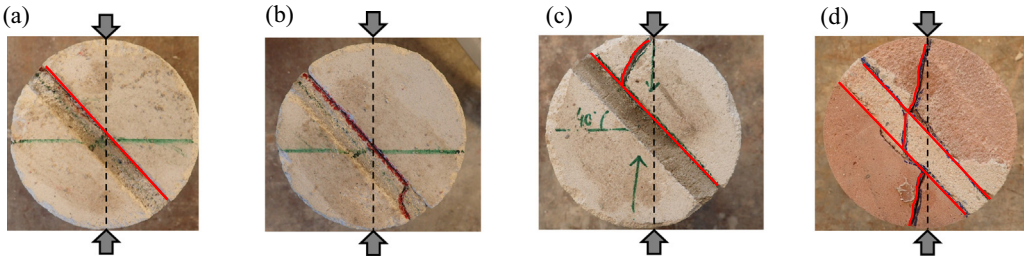

Fig. 6. Typical failure mode of cores under shear load: (a) shear-sliding failure along one interface ("S"); (b) shear-sliding failure along two interfaces including mortar failure ("S"); (c) mixed sliding-tensile failure ("ST"); (d) tensile failure ("T").

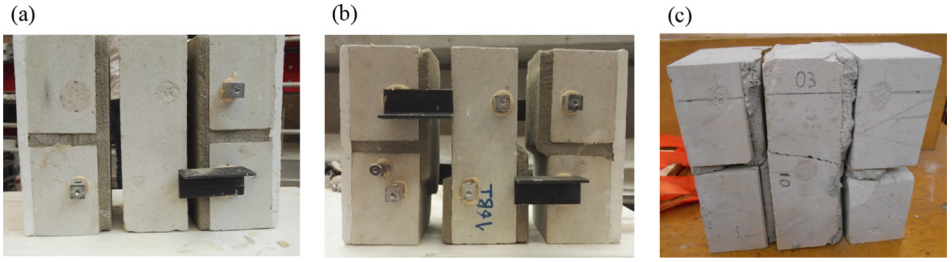

Fig. 7. Typical failure of triplets under shear-compression loading: (a) shear-sliding failure along one interface ("S"); (b) shear-sliding failure along two interfaces ("S"); (c) tensile failure of the middle brick ("T").

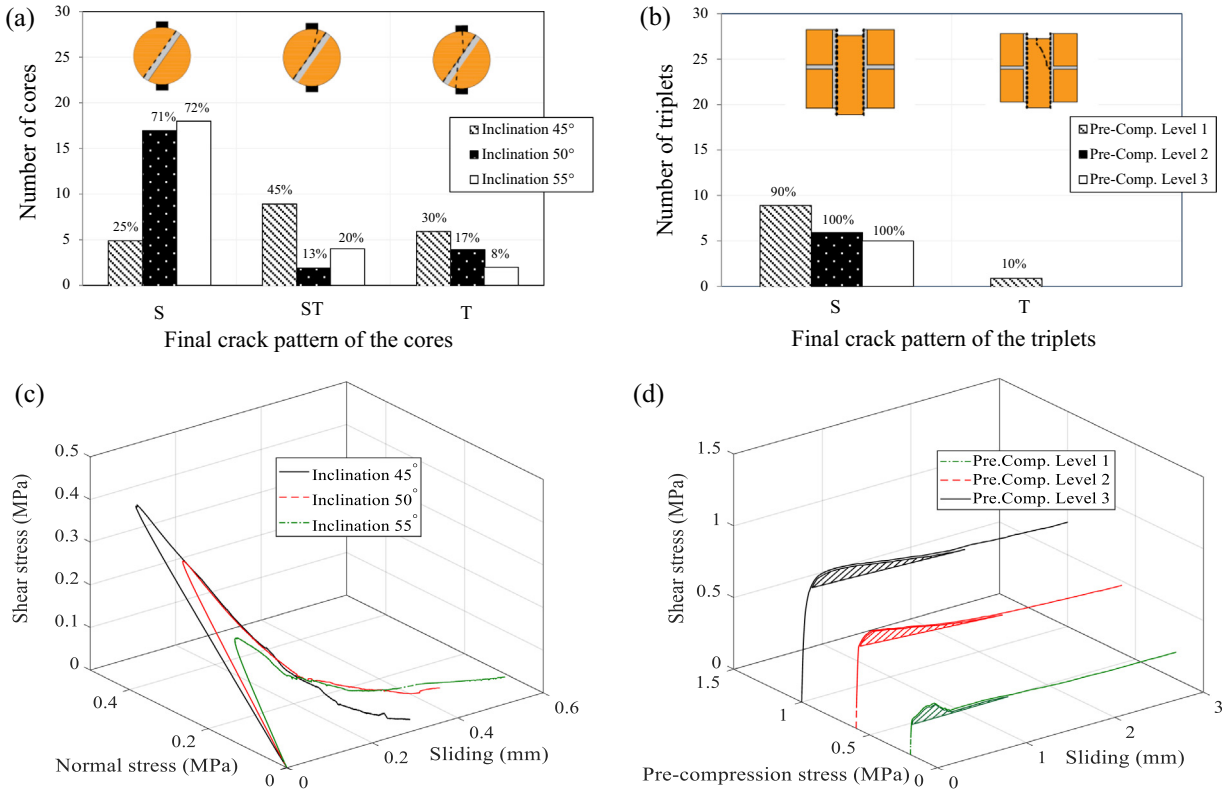

Fig. 8. Overview of different failure modes with respect to the number of cores (a) and number of triplets (b); typical mean stress-sliding relationship observed during shear tests on the cores (c); and shear-compression tests on triplets (d). The number of cores and triplets were counted independently of the objects.

cohesion of the Rengersweg object compared with the others. This confirms the assumption of a strong bond leading to the tensile failure mode ("T") of the core. This may result in limiting the applicability of the core testing method. Accordingly, further experimental and numerical investigations are suggested to clarify the possible influence of mortar properties on the applicability of the core testing method.

The final crack pattern of the cores and of the triplets may be influenced by the imposed inclination angles and the pre-compression levels, respectively (Fig. 8a,b). The occurrence of

shear-sliding failure ("S") was more pronounced when cores were tested at the highest inclination angle (55°). However, testing the cores at the lowest inclination angle (45°) increased the probability of the mixed failure mode ("ST" and "T"). With regard to the triplets, when the pre-compression level was increased, the failure mode was mostly governed by failure along two interfaces rather than the failure along one interface that prevailed for the lowest pre-compression level.

Because a dissimilar boundary and loading conditions were imposed, the shear stress-sliding curves obtained from the two testing methods showed similarities as well as differences. In the pre-peak phase, the mean shear stress-sliding curves obtained from the two testing methods is characterised by linear behaviour up to a stress of approximately 35–60% of the peak stress, followed by a nonlinear branch until the peak load was reached (Fig. 8c,d). The maximum values of the shear and normal stress for the cores could be considered a function of the inclination angle (Table 2). At the inclination angle of 45°, the normal component had the same magnitude as the shear one; however, when the inclination angle was increased, the normal stress had a lower magnitude than the shear stress. As is frequently observed, the higher the value of the mortar joint inclination angle, the lower the values of the shear and the normal strength. In the post-peak phase, both testing methods showed softening behaviour caused by damage and wear of the asperities along the brick–mortar interface. In this phase, the mean shear stress-sliding curves obtained from both methods could be approximated with an exponential curve. With an increase in the plastic shear-sliding deformation of the cores, both the shear and normal stress progressively decreased to a zero value. Note that when using the sliding-controlled set-up, full gradual post-peak softening behaviour was obtained only for the cores with pure shear-sliding failure (i.e. "S"). However, the post-peak phase of the cores with the mixed sliding-tensile failure (i.e. "ST") was not or only partially recorded. Unlike the cores with variable normal stress, the pre-compression stress on the triplets was kept constant during the entire test. Accordingly, after the occurrence of decohesion in the triplets (representing mode-II cohesion softening), no further reduction in the shear stress was found due to the presence of friction. Generally, with the increase in pre-compression stresses in the triplets, the transition of the shear stress from peak strength to zero cohesion became smoother.

To capture the gradual post-peak softening of the cores, and thus to avoid sudden instability, control of the shear-sliding deformations along the interface of the core is required rather than control of the displacement of the jack. Due to the stable propagation of the shear crack, the internal measuring system of the jack showed snap-back behaviour (Fig. 9a), meaning that the masonry relaxes along the load lines while the shear crack propagates in a stable manner. Contrary to this, the LVDTs on the cores always showed a progressive sliding deformation. Although the snap-back behaviour occurred during the shear-sliding failure along the brick-mortar interface, it was not as pronounced as was reported by van der Pluijm [41] and Rots [43] for other cases with tension or shear cracking. In the case of triplets, both the LVDTs and jack measuring system showed an increase in sliding deformation, because the applied pre-compression load prevented any lateral instability (Fig. 9b). Due to the inherent stiffness of the testing set-up, the deformations measured by the jack differed from the measurement by the LVDTs; however, only the LVDT recording was considered.

4. Cohesion and friction coefficient

The Coulomb failure criterion was used to estimate the shear strength properties, as both cores and triplets showed shear-sliding failure along the brick-mortar interface. Accordingly, the cohesion (initial shear strength) and the friction coefficient obtained from both testing methods provided a basis for comparison. To this end, a database was created (Table 2) that included the results of the seven objects investigated in this study along with data from the literature on two replicated clay masonry objects [21,23]. As mentioned in Section 3, all the specimens that showed the tensile failure mode "T" were excluded from the analysis.

To directly correlate the shear properties of the two testing methods, a linear regression analysis was performed on the nine masonry objects. For this reason, the values for cohesion and the initial friction coefficient obtained from the shear test on the cores were plotted against the values obtained from the triplet tests (Fig. 10). The regression line, forced to pass through the origin, is shown as a black solid line. A one-to-one correlation line (the red dashed line) is also added to Fig. 10, while the grey area indicates the scatter band. The errors, calculated as the deviations with respect to the regression lines, are also presented.

The regression analysis indicates that there is an acceptable statistical relationship both in terms of cohesion and friction coefficient regardless of masonry types, where the shear property values of the triplets were found to be approximately 0.90 times lower than the ones obtained from the core tests. In addition, low dispersion of the shear properties can be observed, as all the experimental results fall within a narrow scatter band (grey area). In conclusion, a minimally invasive core testing method can be regarded as a reliable alternative to the conventional triplet and shove test method for evaluating the shear strength properties of existing structures.

5. Elastic shear modulus of the mortar joint

Large scatter was found in the mortar shear modulus by performing tests on the cores. This was attributed to the heterogonous nature of masonry, which may cause complex distribution of stress along the joint even in the elastic phase (see Table 2). Due to the lack of data for the triplet tests, a direct comparison of the results with those from the core tests could be made for only two objects,

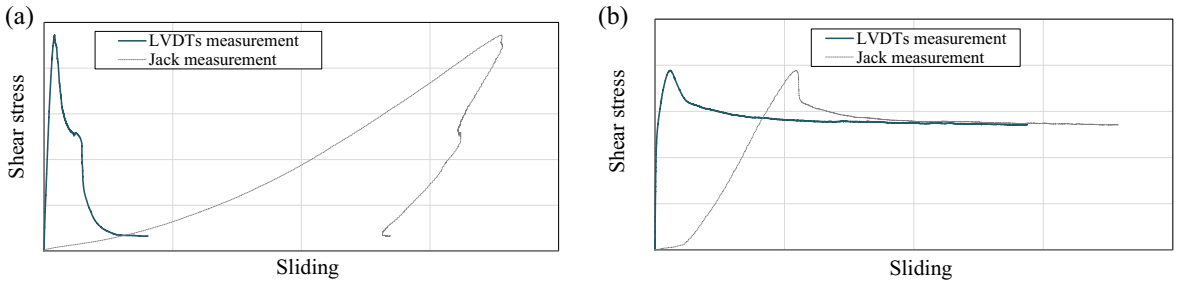

Fig. 9. Typical shear stress-sliding curve obtained from the jack and LVDT measurements: (a) shear test on core with sliding-controlled set-up; (b) shear-compression test on triplet with displacement-controlled set-up.

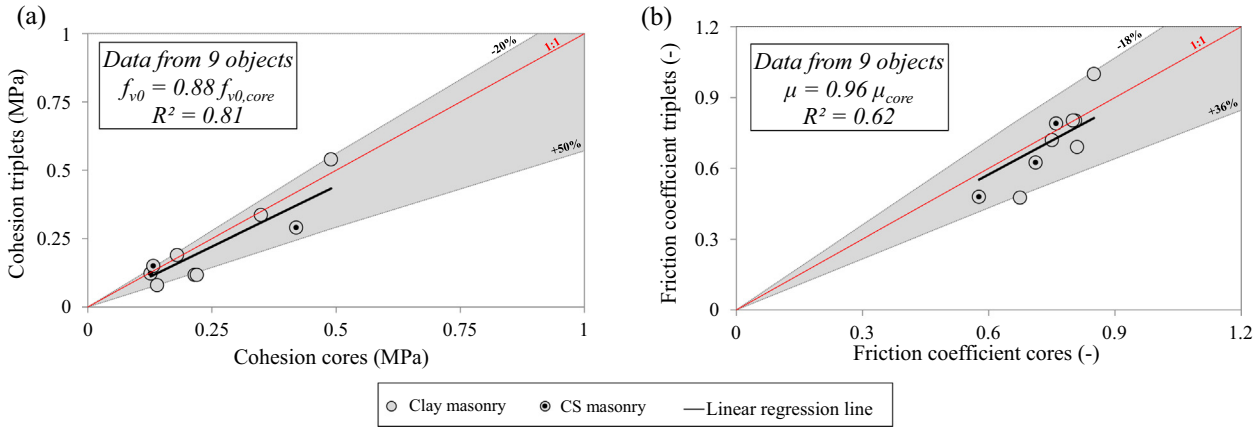

Fig. 10. Correlation between shear properties of cores and of companion specimens: (a) cohesion; (b) friction coefficient. The shaded grey area identifies the scatter band. The errors, which are the deviations with respect to the regression line, are reported.

namely the CS masonry from the Tilweg building, and the replicated clay masonry MAT-4. For these two objects, the variation in mean shear modulus in the pre-peak phase as a function of normalized shear stress is shown in Fig. 11. For each testing method, the mean shear modulus curve was found by evaluating the average results of every single specimen with the shear-sliding ("S") and mixed sliding-splitting failure mode ("ST"), regardless of the imposed inclination angle or the pre-compression level. The shear stress was normalized with respect to the shear strength. At the very beginning of the tests, the resolution of the measuring system could have had an effect on the accuracy of the measured sliding; accordingly, the shear modulus was reported only for normalized shear stresses higher than 0.2. The mean shear modulus curves of the cores and of the triplets are presented with a solid line and a dashed line, respectively. The corresponding 95% confidence intervals based on a Gaussian distribution are also presented [25].

An acceptable correspondence between the elastic shear stiffness of the two methods was found, although with an increase in the shear stress, the shear modulus of the cores decreased at a higher rate than that of the triplets (Fig. 11). Such a difference in the response of the two testing methods can be attributed to the different boundary conditions imposed, as shear cracks developed at a lower rate in the pre-compressed triplets than in the cores with the constant change in the normal stress. The ratio of the shear modulus of the triplets to the cores at a stress level corresponding to 1/3 of the maximum shear stress ranges from 1.1 to 1.3 (Fig. 11), although this comparison was made for only two masonry objects. This finding brings to light the potential of shear tests on cores to address the elastic shear modulus of the mortar joint; however, further research is required to draw concrete conclusions.

6. Fracture energy for shear-sliding cracking

To evaluate the dissipated energy during the formation of the shear crack linked to the cohesive mechanisms, the frictional contribution arisen from the surface roughness along the brick–mortar interface is excluded. In other words, the notion behind the fracture energy in shear is to distinguish the cohesion mechanism from the contribution of friction, see Fig. 5 in Section 2.3**.** For both cores and triplets, the variations in the fracture energy of cores as a function of maximum normal stress ($f_{p,core}$) and of triplets as a function of pre-compression stress (f_p) are plotted in Fig. 12. To illustrate this trend, the linear regression line for each given masonry type is also added.

With an increase in the maximum normal stress, the fracture energy in the cores consistently followed a downward trend, while no clear trend was observed from the results of the triplet tests (Fig. 12). Regarding the trends of fracture energy, a comparison between the two testing methods can be made for only two objects, namely the CS masonry from the Tilweg and Zijlvest buildings. The cores and triplets taken from the Tilweg object showed a

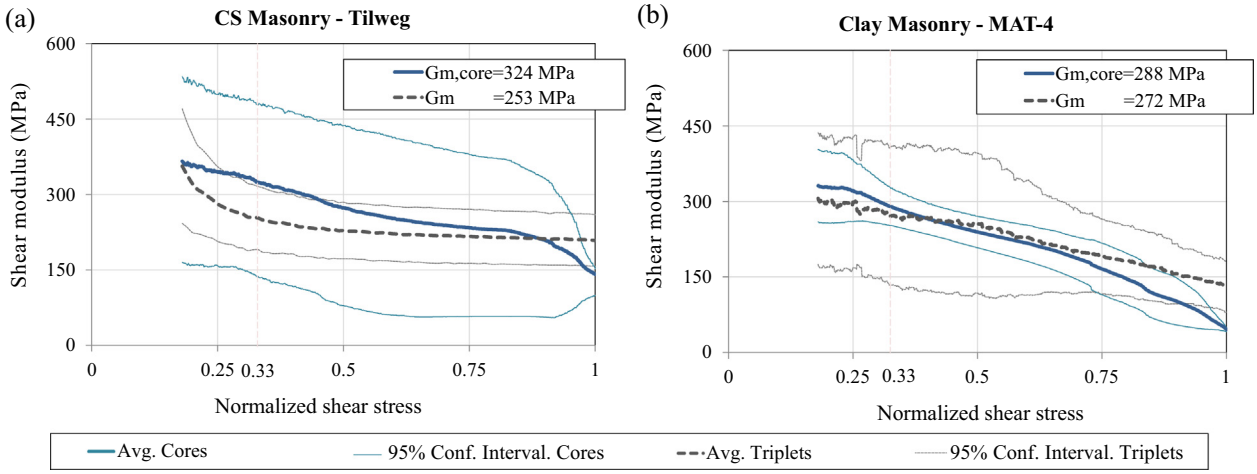

Fig. 11. Variation in the shear modulus of the mortar joint as a function of normalized shear stress: (a) existing CS masonry Tilweg; (b) replicated clay masonry MAT-4.

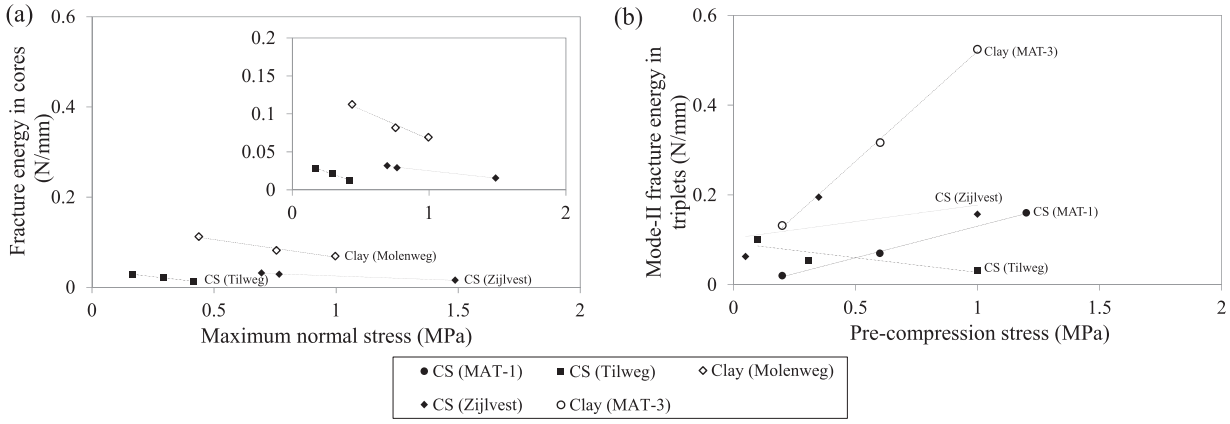

Fig. 12. Variations in the values of fracture energy as a function of: (a) maximum normal stress in cores; (b) pre-compression stress in triplets.

similar trend in which an increase in normal stress was accompanied by a decrease in fracture energy. However, for the Zijlvest object, an inconsistency between the trends of the fracture energy in the cores and triplets was obvious. At this time, no potential explanation for such discrepancy can be offered, thus further research is suggested.

The clay masonry clearly showed higher values of energy dissipation than the CS masonry. This observation is in line with the van der Pluijm findings [41], where at a constant pre-compression level of 1.0 MPa, the fracture energy of clay specimens (0.19 N/mm) was almost four times higher than that for CS masonry (0.05 N/mm). For shear-sliding failure along the interface, the CS specimens, both cores and triplets, often showed a smoother crack surface than did the clay specimens (Fig. 13). This may explain why less energy was required to create a shear crack at the brick–mortar interface of the CS masonry than was required by the clay masonry specimen.

Although fracture energy is commonly acknowledged as a size-independent property, in this study, as in previous studies (e.g. [40,49]), a clear dependency of the mode-II fracture energy on pre-compression levels was observed. The triplets showed variation in the mode-II fracture energy up to 85% (with respect to an average value of fracture energy). On the contrary, for the cores, a nearly constant trend in fracture energy with respect to the maximum normal stress was obtained, with a maximum variation of approximately 38%. These conflicting observations pose a challenging question: is the mode-II fracture energy in masonry an independent property or not? It should be pointed out that the definition of mode-II fracture energy remains a debatable issue for quasi-brittle material, as shown by several discussions in the field of concrete material. Bazant et al. [50] explained that breaking the interlocking of concrete aggregate due to shear resistance requires an energy that is almost 25 times larger than the tensile (mode-I) fracture energy. On the contrary, Carpinteri et al. [51] stated that for mixed mode crack propagation, mode-I fracture energy can be obtained by excluding the energy dissipation due to the friction and interlocking of concrete aggregate. In addition, they observed that the energy dissipation due to the interlocking of aggregate and asperities disappeared with the increase in specimen size as well as the decrease in aggregate size. Furthermore, Carpinteri et al. [51] reported on the dependency of mode-II fracture energy to specimen geometry (i.e. size and shape), loading and testing conditions, and thus concluded that mode-II fracture energy in concrete is not a real material property. To produce an answer, extensive research in this realm is suggested.

Although the dissipated energy during the formation of shear cracks in both cores and triplets can be considered to be fracture energy, due to the influence of the lateral boundary conditions, there is a substantial difference between them. Throughout the shear-compression tests on triplets, the confinement level was kept constant, while during the core tests, the level of confinement decreased in the post-peak phase due to the reduction in the stress state along the joint. Considering such differences in the boundary conditions of the two testing methods, no direct comparison can be made in terms of energy dissipation. As found in Section 4, an acceptable correspondence was found between the failure criteria of the two testing methods. For this reason, an attempt was made to extrapolate the post-peak softening behaviour of the triplets using the data gathered from the core tests. For the triplets, the descending cohesive branch beyond the peak shear stress can be approximated by an exponential curve. As introduced by van der Pluijm [41], the post-peak response can be predicted as:

$$c_p = c_{core}.e^{-\frac{c_{core}.\delta_p}{G_{f,avg(core)}}} \quad (6)$$

where c_p is the post-peak cohesive stress, c_{core} is the maximum cohesive stress (Fig. 5), $G_{f,avg(core)}$ is the average value of the fracture energy in the cores at different inclination angles, and δ_p is the predicted shear-sliding deformation in the post-peak phase. The steps taken to find the analytical post-peak softening of the triplets based on the data obtained from core tests are as follows:

1. The shear strength was retrieved at three given pre-compression levels using the Coulomb failure criterion established from the core tests,

Fig. 13. Top view from the debonded surface of CS and clay masonry specimens: (a-b) cores; (c-d) triplets.

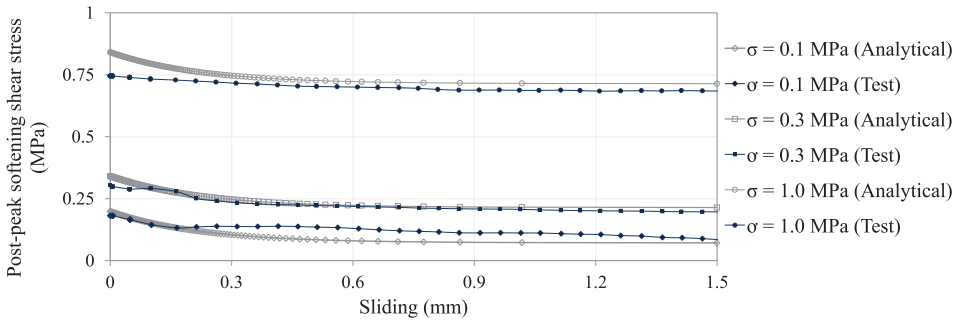

Fig. 14. Comparison between the experimental post-peak softening during the shear-compression tests on triplets and the analytical model extrapolated from the core tests on the CS Tilweg object.

2. The residual friction strength was calculated by multiplying the given pre-compression stress by the friction coefficient obtained from the core tests,
3. The maximum cohesive stress (c_{core}) was found by subtracting the residual shear strength from the peak shear stress (please note that c_{core} as defined here will be the same as the one in Fig. 5c if $f_{p,core} = f_p$),
4. The post-peak cohesive stress (c_p) was defined by dividing the maximum cohesive stress over 100 equal steps in descending order,
5. The corresponding predicted sliding (δ_p) was found from Eq. (6), considering c_{core}, c_p, and $G_{f,avg(core)}$ as inputs. The fracture energy in the cores did not vary significantly when the inclination angle was changed. Accordingly, for the sake of simplicity, the fracture energy was assumed to be constant and was calculated as an average value of the fracture energy at different inclination angles.
6. The post-peak shear stress corresponding to the sliding was found as the sum of the post-peak cohesive stress and the residual shear strength.

In Fig. 14, a comparison is made between the experimental and analytical results in terms of the post-peak behaviour of the triplets. Note that the comparison could be made for only two objects, namely the CS masonry from the Tilweg and Zijlvest buildings; however, the data of the latter object were excluded due to insufficient testing and the wide spread of the testing results. At pre-compression levels of 0.10 MPa and 0.30 MPa, there is an acceptable correspondence between the post-peak softening from the experiment and the analytical calculation. However, at the highest pre-compression level, the shear stress decreases at a lower rate than the analytical calculation. This difference can be traced back to the disagreement between the failure criteria of the two testing methods. In conclusion, the core testing shows some potential for evaluating the post-peak softening, though this conclusion is derived based on the results for only one object.

7. Dilatant behaviour

The volumetric normal expansion of the masonry bed joint during the shear-sliding deformations was measured for both cores and triplets. For a given inclination angle or pre-compression level, the mean values of dilatancy as a function of normalized sliding are presented in Fig. 15. The sliding was normalized with respect to the sliding that corresponded to the maximum shear stress. To compare the results of the two testing methods, only half of the normal displacement measured across the two bed joints was considered for the triplet tests. As mentioned in Section 2.3, the dilatancy was evaluated over the constant sliding increment, and the corresponding normal deformations were subsequently found. Herein, for the sake of consistency, the increment was defined as 0.25 times the sliding corresponding to the peak shear stress; this increment was regarded as sufficiently small to qualitatively capture the trend. Note that the normal expansion of the joint was recorded only for the cores extracted from the four existing buildings (i.e. Tilweg, Zijlvest, Molenweg, and Rengersweg) and for the triplets replicated in the laboratory (i.e. MAT-1, MAT-3), and was

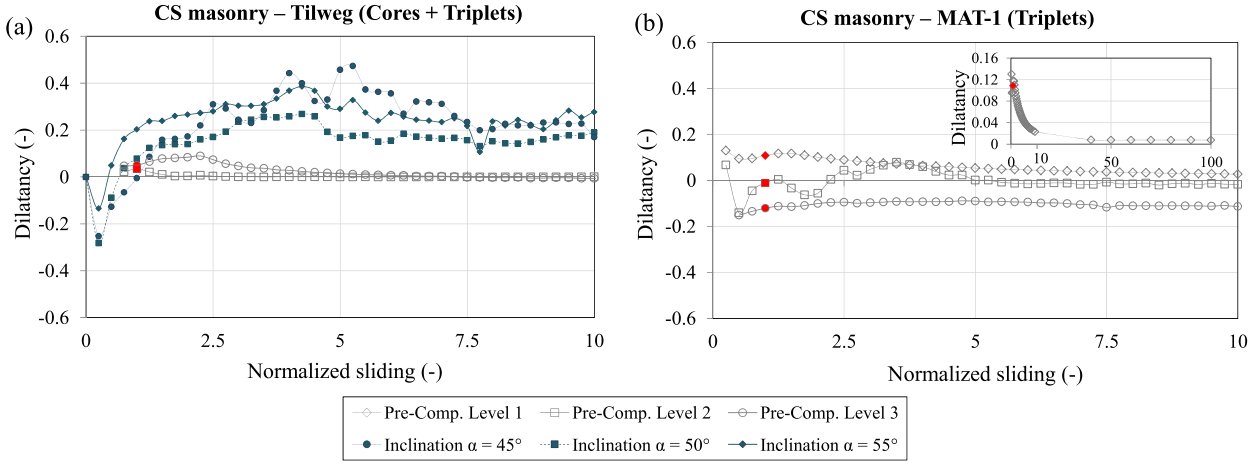

Fig. 15. Dilatancy versus normalized sliding: (a) existing CS masonry, Tilweg; (b) replicated CS masonry, MAT-1. The sliding was normalized with respect to the sliding occurred at maximum shear stress, as indicated with a red marker. (For interpretation of the references to colour in this figure legend, the reader is referred to the web version of this article.)

Table 3
Summary of the shear properties of standard triplets and modified triplets for two replicated objects.

	CS masonry MAT-1			Clay masonry MAT-3		
Pre-compression level (MPa)	0.20	0.60	1.20	0.20	0.60	1.00
Standard triplets						
Number of specimens	3	3	3	2	2	2
Shear strength (MPa)	0.19	0.45	0.71	0.32	0.65	0.88
C.o.V	8%	3%	4%	17%	12%	19%
Modified triplets						
Number of specimens	3	3	3	3	2	3
Shear strength (MPa)	0.27	0.46	0.72	0.29	0.58	0.93
C.o.V	22%	8%	3%	29%	9%	8%
Standard triplets + Modified triplets						
Shear strength (MPa)	0.21	0.46	0.71	0.30	0.61	0.91
C.o.V	13%	5%	3%	23%	11%	15%

extracted only from the Tilweg building. As a result, a comparison between the dilatant response of the cores and the triplets can be made for only one object, namely the CS masonry from the Tilweg building (Fig. 15a). For all the investigated masonry types, a similar trend of variations in dilatancy over the normalized sliding was found as presented in Fig. 15a-b.

No specific trend was detected between the progressive normal expansion of the cores and the imposed inclination angles, while the lateral expansion of the triplets depended on the pre-compression levels. As mentioned earlier, the confinement condition of the two testing methods in the direction perpendicular to the bed joint differed. Accordingly, in the post-peak phase, with the decrease in the stress state in the cores, the lateral confinement constantly decreased, and the joint expanded more easily. The three sets of mean dilatancy curves obtained from the tests on the cores at different inclination angles clearly followed the same trend (Fig. 15a). First, a contraction of the mortar joint was observed. With the increase in sliding deformation, the joint tended to expand progressively. A turning point was found at a normalized sliding of approximately 0.25. Eventually, at larger values of sliding, due to wear and damage to the asperities along the brick–mortar interface of the unconfined cores, the dilatancy became stable at a non-zero value. The dependence of dilatancy on the pre-compression level was observed in tests on the triplets; the lower the pre-compression level, the higher the dilatancy. At the highest pre-compression level, the dilatant behaviour in the triplets was either not observed or vanished at a higher rate as the damage to the fracture surface accelerated. In addition, the roughness of the brick surface played an important role in the dilatancy effect [44]. It should be pointed out that all the triplets showed dilatant behaviour, with the exception of the replicated CS triplets tested at a pre-compression level of 1.2 MPa (see Fig. 15b). In conclusion, the lateral expansion of the cores, with constant change in the normal stress, was greater than that of the triplets with constant pre-compression. Accordingly, by further increasing the shear-sliding deformation along the brick–mortar interface, the dilatant behaviour of the cores remained stable, while the dilatant behaviour of the triplets progressively vanished.

8. Conclusions

Through a comparative experimental approach, this study examined the suitability of shear tests on small-diameter cores to assess nonlinear shear-sliding behaviour along a brick-mortar interface. For this purpose, an experimental program was set-up at Delft University of Technology to compare the results obtained from shear tests on cores and from triplet tests on seven masonry objects. The masonry objects were either replicated in the laboratory or extracted from residential buildings located in the northern part of the Netherlands (Groningen area). The boundary condition imposed in the direction perpendicular to the bed joint of the core was different from that of the triplets, as the level of confinement in the core was not constant throughout the test, while during the triplet test the confinement level was kept constant. Cores with a diameter of 100 mm and composed of a single bed joint were rotated with respect to their original horizontal position and subsequently subjected to vertical line load along their thickness, similar to a Brazilian splitting test. The test was carried out at different inclination angles of 45°, 50°, and 55°, thus inducing various combinations of shear-compression stress states along the brick-mortar interface. Unlike previous research, in this study a sliding-controlled set-up was also used to characterise the post-peak softening behaviour. Consequently, a more complete description of the nonlinear shear-sliding behaviour along the brick-mortar interface was provided in terms of cohesion, friction coefficient, shear modulus of the mortar joint, as well as some insight into shear softening, energy dissipation, and dilatancy.

The failure of the cores under shear load can be influenced by the imposed inclination angle and can also be affected by the mortar strength and bond strength of the interface, which introduces limitations in the application of the core testing method to determine the shear-sliding behaviour at a brick-mortar interface. At the highest inclination angle (55°), 83% of the cores failed along the brick-mortar interface, while at the lowest inclination angle (45°), the number of cores that showed pure shear-sliding failure dropped to 25%. For this inclination angle, 45% of the cores failed with mixed shear-sliding and brick splitting failure, and the remaining 30% showed tensile failure, characterised by an evident vertical crack aligned with the loading axis and a shear-sliding crack along the interface. The results of tensile failure could not be regarded as representative of shear-sliding behaviour, and thus were excluded from the evaluation of the shear properties. The presence of the tensile-splitting failure mode was attributed to the homogeneous performance of the masonry, which was due to the good quality mortar or/and good bond at the brick–mortar interface. Accordingly, the accuracy of the obtained results from the core testing method can be questioned with respect to the observed failure mode and masonry characteristics. With this in mind, further research is suggested to investigate the range of applicability of the core testing method for masonry with a strong bond as well as for masonry with different ratios of stiffness of the mortar to the brick.

This study confirms the suitability of the core testing method in assessing the cohesion and friction coefficient of brick masonry. To predict a relationship between the cohesion obtained from the two testing methods as well as the friction coefficient, a regression analysis was performed on nine masonry objects, including data form the literature. As derived from this analysis, the cohesion of

the triplets was found to be 0.88 times lower than that of the cores with a strong correlation (R^2 = 0.81). The friction coefficient of the triplets was found to be 0.96 times lower than the friction coefficient of the cores with a moderate correlation (R^2 = 0.62).

In the elastic phase, the core testing method shows the potential for evaluating the shear modulus of the mortar joint, although the comparison between the outputs of the two testing methods applies to only two masonry objects. Accordingly, with the aim of augmenting the established dataset, further studies are suggested. In general, tests on the cores resulted in a large scattering of the shear modulus that could be attributed to the heterogeneous nature of the masonry.

Unlike previous studies, this paper provides a comparison of core and triplet tests in terms of mode-II fracture energy. In both tests, the energy dissipation is governed by cohesive and friction mechanisms. To consider only the cohesive contribution associated with shear cracking, the friction contribution determined as the product of the normal stress and the friction coefficient was subtracted from the shear stress. The fracture energy was then calculated as the area under the cohesive shear stress-sliding curve. Unlike the triplets, the cores showed a nearly constant trend between the mode-II fracture energy and the maximum normal stress. For one masonry type, an acceptable agreement was found between the post-peak softening of the triplets predicted using the core testing results and the experiments. The difference between the cores and the triplets in terms of mode-II fracture energy and the dependency of the mode-II fracture energy of the triplets on the pre-compression stress raises some doubt about this parameter as an independent material property. Nevertheless, the comparison between the two testing methods points to a new research direction.

Due to the difference in the lateral confinement of the bed joint during the shear sliding, the cores showed larger dilatancy than the triplets did. In the post-peak phase, with the decrease in the stress state in the cores, the lateral confinement constantly decreased, and the joint expanded more easily, while in the triplets the lateral confinement was kept constant throughout the test. By increasing the shear-sliding, the dilatancy of the cores gradually decreased and eventually reached a steady non-zero value. The same trend was observed for the cores tested under different inclination angles. With the increase in the pre-compression level and the sliding, the dilatancy behaviour of the confined triplets slowly vanished and almost reached zero. However, understanding the influence of boundary conditions on shear properties involves an extensive debate (e.g. [15,17,41–45]).

This study confirms that the applicability of the core testing method can be extrapolated to both clay and CS brick masonry types extracted from existing URM buildings. It was observed that the reliability and the variability of the experimental results were not influenced by the brick types, i.e. clay or CS brick masonry, or construction types, i.e. laboratory-made or field-extracted. However, the results were influenced by the mortar properties. From the perspective of in-situ application, the core testing method can be regarded as a reliable alternative to conventional standardized methods, such as triplet and shove tests, as far as evaluations of shear strength and shear stiffness are concerned, while evaluations of the softening parameters and dilatancy require further study.

CRediT authorship contribution statement

Samira Jafari: Conceptualization, Methodology, Validation, Data curation, Writing - original draft. **Jan G. Rots:** Conceptualization, Writing - review & editing, Supervision, Funding acquisition. **Rita Esposito:** Conceptualization, Writing - review & editing, Supervision, Funding acquisition.

Data for reference

The experimental results of the presented tests are available via the 4TU.ResearchData repository at http://doi.org/10.4121/uuid:63bad069-2d7c-4e4d-9f91-c41b29605fc7. The data are distributed under the license type CC BY.

Declaration of Competing Interest

The authors declare that they have no known competing financial interests or personal relationships that could have appeared to influence the work reported in this paper.

Acknowledgment

This research was funded by Nederlandse Aardolie Maatschappij (NAM), under contract numbers UI46268 “Physical testing and modelling – Masonry structures Groningen” (contract holders Jan van Elk and Jeroen Uilenreef) and UI63654 “Testing program 2016 for Structural Upgrading of URM Structures” (contract holders Dick den Hertog and Reza Sarkhosh), which is gratefully acknowledged. The authors are thankful to the staff of the TU Delft Macrolab/Stevinlaboratory and to M.Sc. students Lucia Licciardello and Elena Casprini for assistance during the tests. The collaboration with engineering company ARUP in extracting samples is acknowledged. The authors acknowledge the collaboration with Dr Ad Vermeltfoort and Prof. Dirk Martens from Eindhoven University of Technology, who performed shear-compression tests on triplets extracted from the Molenweg building, and the collaboration with engineering company B|A|S, who performed shear-compression tests on triplets extracted from the Rengersweg building.

Appendix A

To study the influence of triplet geometry on shear properties, both standard triplets (stacked-bonded triplets) and modified triplets (half-bonded triplets) were constructed in the laboratory. Shear-compression tests on triplets were generally performed on standard triplets following EN 1052-3:2002 [10]. In the case of existing buildings with a running bond, half-bonded specimens, including two head joints, were extracted for testing purposes (Fig. A.1a).

For the two masonry objects replicated in the laboratory, the difference between the Coulomb failure criterion of the standard triplets and of the modified triplets is shown in Fig. A.2 and Table 3. Considering all the results obtained by the standard and modified triplets, no significant statistical difference was found for CS masonry at any imposed pre-compression level, as the coefficient of variation ranged from 3% to 13%. On the contrary, the shear strength of the clay modified triplets differed slightly from that

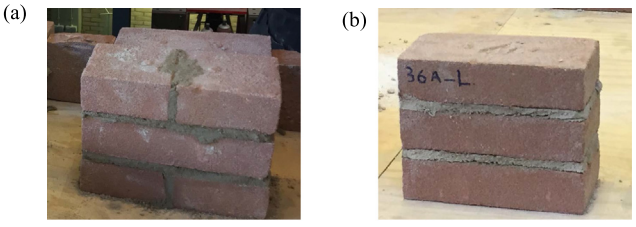

Fig. A.1. Laboratory made triplets: (a) modified triplets; (b) standard triplets.

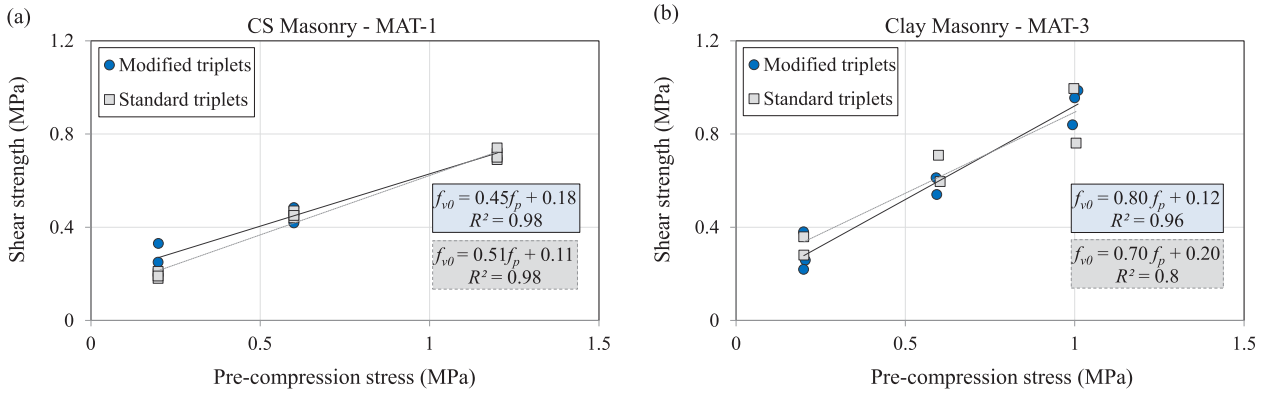

Fig. A.2. Comparison between shear properties of the standard and modified triplets: (a) replicated CS masonry MAT-1; (b) replicated clay masonry MAT-3.

of the standard triplets; the coefficient of variation was between 11% and 23%. Because these results were found from tests on a limited amount of data, further experimental and numerical study is suggested to fully comprehend the impact of the head joint on the shear-sliding behaviour.

References

[1] H. Lotfi, P. Shing, An appraisal of smeared crack models for masonry shear wall analysis, Comput. Struct. 41 (3) (1991) 413–425.
[2] P.B. Lourenço, J.G. Rots, J. Blaauwendraad, Continuum model for masonry: parameter estimation and validation, J. Struct. Eng. 124 (6) (1998) 642–652.
[3] L. Gambarotta, S. Lagomarsino, Damage models for the seismic response of brick masonry shear walls. Part I: the mortar joint model and its applications, Earthquake Eng. Struct. Dyn. 26 (4) (1997) 423–439.
[4] S. Marfia, E. Sacco, Multiscale damage contact-friction model for periodic masonry walls, Comput. Methods Appl. Mech. Eng. 205 (2012) 189–203.
[5] P.B. Lourenço, J.G. Rots, Multisurface interface model for analysis of masonry structures, J. Eng. Mech. 123 (7) (1997) 660–668.
[6] A.M. D'Altri, F. Messali, J. Rots, G. Castellazzi, S. de Miranda, A damaging block-based model for the analysis of the cyclic behaviour of full-scale masonry structures, Eng. Fract. Mech. 209 (2019) 423–448.
[7] A. Anthoine, G. Magonette, G. Magenes, editors. Shear-compression testing and analysis of brick masonry walls. In: 10th European Conference on Earthquake Engineering; 1995.
[8] M. Tomaževič, M. Lutman, L. Petković, Seismic behaviour of masonry walls: experimental simulation, J. Struct. Eng. 122 (9) (1996) 1040–1047.
[9] G. Magenes, G.M. Calvi, In-plane seismic response of brick masonry walls, Earthquake Eng. Struct. Dyn. 26 (11) (1997) 1091–1112.
[10] EN 1052-3. Methods of test for masonry - Part 3: Determination of initial shear strength. 2002.
[11] ASTM C1531. Standard test methods for in situ measurement of masonry mortar joint shear strength index. American Society for Testing and Materials (ASTM) International, 2016.
[12] L. Binda, C. Tiraboschi, Flat-jack test: a slightly destructive technique for the diagnosis of brick and stone masonry structures, Restoration Build. Monuments 5 (5) (1999) 449–472.
[13] E. Cescatti, M. Dalla Benetta, C. Modena, F. Casarin, editors. Analysis and evaluations of flat jack test on a wide existing masonry buildings sample. 16th International Brick & Block Masonry Conference; 2016: CRC Press London, UK.
[14] F. Graziotti, G. Guerrini, A. Rossi, G. Andreotti, G. Magenes, Proposal for an Improved Procedure and Interpretation of ASTM C1531 for the in Situ Determination of Brick-Masonry Shear, Strength (2018), https://doi.org/10.1520/STP161220170181. https://compass.astm.org/DIGITAL_LIBRARY/STP/PAGES/STP161220170181.htm.
[15] G. Andreotti, F. Graziotti, G. Magenes, Detailed micro-modelling of the direct shear tests of brick masonry specimens: the role of dilatancy, Eng. Struct. 168 (2018) 929–949.
[16] F. Ferretti, S. Jafari, R. Esposito, J.G. Rots, C. Mazzotti, editors. Investigation of the shear-sliding behaviour of masonry through shove test: experimental and numerical studies, in: 11th International Conference on Structural Analysis of Historical Constructions; 2018; Cusco, Peru: Springer.
[17] G. Andreotti, F. Graziotti, G. Magenes, Expansion of mortar joints in direct shear tests of masonry samples: implications on shear strength and experimental characterization of dilatancy, Mater. Struct. 52 (4) (2019) 64.
[18] E.C. Manning, L.F. Ramos, F. Fernandes, editors. Tube-jack testing: Semi-irregular masonry wall testing. 10th International Conference on Structural Analysis of Historical Constructions; 2016 12-16 September; Leuven, Belgium: Taylor & Francis Group, London.
[19] F. Braga, M. Dolce, B. Filardi, A. Masi, D. Nigro. A test method to assess the shear strength of existing masonry structures-Theoretical basis and first experimental results. Int Work CNR-GNDT Effectiveness of Injection Techniques for Retrofitting of Stone and Brick Walls in Seismic Areas; Milan, Italy1992. pp. 204–27.
[20] A. Benedetti, L. Pelà, A. Aprile, editors. Masonry properties determination via splitting tests on cores with a rotated mortar layer. Proceedings of 8th International Seminar on Structural Masonry, Istanbul, Turkey; 2008.
[21] A. Benedetti, L. Pelà, editors. Experimental characterization of mortar by testing on small specimens. 15th International Brick & Block Masonry Conference; 2012.
[22] C. Mazzotti, E. Sassoni, G. Pagliai, Determination of shear strength of historic masonries by moderately destructive testing of masonry cores, Constr. Build. Mater. 54 (2014) 421–431.
[23] L. Pelà, K. Kasioumi, P. Roca, Experimental evaluation of the shear strength of aerial lime mortar brickwork by standard tests on triplets and non-standard tests on core samples, Eng. Struct. 136 (2017) 441–453.
[24] L. Pelà, P. Roca, A. Benedetti, Mechanical characterization of historical masonry by core drilling and testing of cylindrical samples, Int. J. Archit. Heritage 10 (2–3) (2016) 360–374.
[25] D. Marastoni, L. Pelà, A. Benedetti, P. Roca, Combining Brazilian tests on masonry cores and double punch tests for the mechanical characterization of historical mortars, Constr. Build. Mater. 112 (2016) 112–127.
[26] S. Jafari, R. Esposito, J. Rots. Literature review on the assessment of masonry properties by tests on core samples, in: 4th WTA International PhD Symposium; 14-16 September; Delft, Netherlands: WTA Nederland - Vlaanderen; 2017.
[27] ASTM C496/C496M-17, Standard test method for splitting tensile strength of cylindrical concrete specimens. 2017.
[28] ASTM E519/E519M-15, Standard test method for diagonal tension (shear) in masonry assemblages. 2015.
[29] S. Jafari, J.G. Rots, R. Esposito, F. Messali, Characterizing the material properties of Dutch unreinforced masonry, Procedia Eng. 193 (2017) 250–257.
[30] B. Zapico Blanco, M. Tondelli, S. Jafari, F. Graziotti, H. Millekamp, J.G. Rots, et al., editors. A masonry catalogue for the Groningen region. 16th European Conference on Earthquake Engineering; 2018 18-21 June; Thessaloniki, Greece.
[31] F. Messali, R. Esposito, S. Jafari, G. Ravenshorst, P. Korswagen, J.G. Rots, editors. A multiscale experimental characterisation of Dutch unreinforced masonry buildings, in: 16th European Conference on Earthquake Engineering; 2018 18-21 June; Thessaloniki, Greece.
[32] R. Esposito, G. Ravenshorst. Quasi-Static Cyclic In-Plane Tests on Masonry Components 2016/2017. Delft, Netherlands: Delft University of Technology, 2017 10 August Report No.: C31B67WP3-4.
[33] R. Esposito, K. Terwel, G. Ravenshorst, H. Schipper, F. Messali, J.G. Rots, editors. Cyclic pushover test on an unreinforced masonry structure resembling a typical Dutch terraced house, in: 16th World Conference on Earthquake; 2017 9-13 January; Santiago, Chile.
[34] ASTM C1532. Standard practice for selection, removal, and shipment of masonry assemblage specimens from existing construction. 2019.
[35] EN 1015-11. Method of test for mortar for masonry – Part 11: Determination of flexural and compressive strength of hardened mortar. 1999.
[36] L. Pelà, P. Roca, A. Aprile, Combined in-situ and laboratory minor destructive testing of historical mortars, Int. J. Architectural Heritage 12 (3) (2018) 334–349.
[37] EN 772-1. Methods of test for masonry units – Part 1: Determination of compressive strength. 2011.
[38] NEN 6790. Technical principles for building structures – TGB 1990 – Masonry structures – Basic requirements and calculation methods. 2005.
[39] S. Jafari, J.G. Rots, R. Esposito, Core testing method to assess nonlinear behavior of brick masonry under compression: a comparative experimental study, Constr. Build. Mater. 218 (2019) 193–205.

[40] S. Stockl, P. Hofmann, J. Mainz, Comparative finite element evaluation of mortar joint shear test, Masonry Int. 3 (3) (1990) 101–104.
[41] R.V. Pluijm, editors. Shear behaviour of bed joints. 6th Canadian Masonry Symposium; 1993 6-9 June Pennsylvania, USA.
[42] F. Ferretti, C. Mazzotti, R. Esposito, J. Rots, editors. Shear-sliding behavior of masonry: numerical micro-modeling of triplet tests. Conference on Computational Modelling of Concrete and Concrete Structures; 2018 February 26 – March 1; Bad Hofgastein, Austria: CRC Press.
[43] J.G. Rots. Structural Masonry: An Experimental/Numerical Basis for Practical Design Rules: AA Balkema; 1997.
[44] G.P. van Zijl, Modeling masonry shear-compression: Role of dilatancy highlighted, J. Eng. Mech. 130 (11) (2004) 1289–1296.
[45] G. van Zijl, J. Rots, A.T. Vermeltfoort, editors. Modelling shear-compression in masonry. Canadian Masonry Symposium; 2001.
[46] L. Pelà, E. Canella, A. Aprile, P. Roca, Compression test of masonry core samples extracted from existing brickwork, Constr. Build. Mater. 119 (2016) 230–240.
[47] A.T. Vermeltfoort. Tests for the Characterization of Original Groningen Masonry under Compression and Shear Loading. Eindhoven University of Technology: Eindhoven University of Technology, 2015 2015. Report No.
[48] S.M. Nonnekes. Masonry Research Report, Location: Rengersweg 11, 9908 PL, Godlinze. Venlo, Netherlands: Research & Technology B|A|S, 2015 15 April. Report No.: 2014-1097-003.
[49] N. Augenti, F. Parisi, Constitutive modelling of tuff masonry in direct shear, Constr. Build. Mater. 25 (4) (2011) 1612–1620.
[50] Z. Bažant, P. Pfeiffer, Shear fracture tests of concrete, Mater. Struct. 19 (2) (1986) 111.
[51] A. Carpinteri, S. Valente, G. Ferrara, G. Melchiorrl, Is mode II fracture energy a real material property?, Comput Struct. 48 (3) (1993) 397–413.